

lin-35/Rb and *xnp-1/ATR-X* function redundantly to control somatic gonad development in *C. elegans*

Aaron M. Bender, Orion Wells, David S. Fay*

Department of Molecular Biology, College of Agriculture, University of Wyoming, Dept. 3944, Laramie, WY 82071, United States

Received for publication 26 December 2003, received 7 May 2004, accepted 9 June 2004

Available online 24 July 2004

Abstract

In screens for genetic modifiers of *lin-35/Rb*, the *C. elegans* retinoblastoma protein (Rb) homolog, we have identified a mutation in *xnp-1*. Mutations in *xnp-1*, including a presumed null allele, are viable and, in general, appear indistinguishable from the wild type. In contrast, *xnp-1 lin-35* double mutants are typically sterile and exhibit severe defects in gonadal development. Analyses of the abnormal gonads indicate a defect in the lineages that generate cells of the sheath and spermatheca. *xnp-1* encodes the *C. elegans* homolog of ATR-X, a human disease gene associated with severe forms of mental retardation and urogenital developmental defects. *xnp-1/ATR-X* is a member of the Swi2/Snf2 family of ATP-dependent DEAD/DEAH box helicases, which function in nucleosome remodeling and transcriptional regulation. Expression of an *xnp-1::GFP* promoter fusion is detected throughout *C. elegans* development in several cell types including neurons and cells of the somatic gonad. Our findings demonstrate a new biological role for Rb family members in somatic gonad development and implicate *lin-35* in the execution of multiple cell fates in *C. elegans*. In addition, our results suggest a possible conserved function for *xnp-1/ATR-X* in gonadal development across species.

© 2004 Elsevier Inc. All rights reserved.

Keywords: *lin-35*; Retinoblastoma; *xnp-1*; ATR-X; *C. elegans*; Development

Introduction

The retinoblastoma protein (Rb) has been shown in multiple systems to be a critical regulator of the cell cycle (reviewed by Kaelin, 1999; Morris and Dyson, 2001). Loss of Rb function, either by direct mutation or through the deregulation of several upstream pathway components, is associated with most human cancers (reviewed by Sherr, 1996; Nevins, 2001). Studies have shown the principal biochemical function of Rb to involve transcriptional repression, namely, transcription factors, such as E2F, recruit Rb to promoter sites (reviewed by Dyson, 1998; Nevins, 1998), whereupon Rb sequesters additional factors

including histone deacetylase (Brehm et al., 1998; Luo et al., 1998; Magnaghi-Jaulin et al., 1998), histone methylases (Nielsen et al., 2001; Pradhan and Kim, 2002; Robertson et al., 2000), and nucleosome remodeling complex components (Dunaief et al., 1994; Strober et al., 1996; Zhang et al., 2000). These factors then collectively alter the local chromatin structure, leading to transcriptional silencing. This latter effect is thought to be the consequence of forming a “closed” chromatin structure, which is less accessible to factors that promote the binding and activation of the RNA polymerase II holoenzyme complex.

The core enzymes involved in the promotion of nucleosome remodeling belong to the Swi/Snf superfamily of ATP-dependent DNA helicases (reviewed by Havas et al., 2001; Sudarsanam and Winston, 2000; Tsukiyama, 2002; Varga-Weisz, 2001). Individual subfamilies, which include the Swi2/Snf2, ISWI, and Mi-2 members, can be distinguished by the presence of signature motifs within the peptide, such

* Corresponding author. Department of Molecular Biology, College of Agriculture, University of Wyoming, Dept. 3944, 1000 East University Avenue, Laramie, WY 82071. Fax: +1 307 766 5098.

E-mail address: davidfay@uwyo.edu (D.S. Fay).

as a bromodomain within the Swi2/Snf2 class. A typical feature of most, though not all Swi/Snf members, is that they function as part of large multisubunit complexes. It is thought that Swi/Snf complexes are (in many cases) recruited to specific promoters through interactions with transcription factors (e.g., Cosma et al., 1999; Wallberg et al., 2000; Yudkovsky et al., 1999). Depending on the context of the promoter, Swi/Snf complexes, once bound, may either activate or inhibit transcription (also see Discussion).

Many specific *in vitro* biochemical activities have been ascribed to Swi/Snf enzymes including binding to naked DNA and nucleosomes (Kingston and Narlikar, 1999; Quinn et al., 1996), looping of DNA (Bazett-Jones et al., 1999), and twisting to generate DNA torsion (Gavin et al., 2001; Havas et al., 2000). Though the precise mechanism is unknown, these activities may lead to three possible outcomes: (1) nucleosome remodeling, whereby structural changes alter the configuration of the “wrapped” DNA and/or the histone octamer (Kingston and Narlikar, 1999; Lorch et al., 1999; Schnitzler et al., 1998); (2) nucleosome sliding, in which nucleosomes are repositioned (with minimal disruption of the histone-DNA complex) along a continuous stretch of DNA (Hamiche et al., 1999; Jaskelioff et al., 2000; Langst et al., 1999; Whitehouse et al., 1999); and (3) trans-displacement, whereby the histone octamer is actually transferred to a separate DNA molecule (Lorch et al., 1999; Owen-Hughes et al., 1996). While much still remains to be solved regarding the precise mechanisms underlying nucleosome movement, even less is currently known about the cellular and developmental functions that most Swi/Snf factors carry out in higher eukaryotes.

Using a genetic approach to identify genes that show synthetic phenotypes in conjunction with the *C. elegans* Rb homolog, *lin-35* (Lu and Horvitz, 1998), we have identified a mutation in *xnp-1*, a conserved member of the Swi/Snf superfamily and homolog of the human gene implicated in ATR-X syndrome (Picketts et al., 1996; Villard et al., 1999). We find that *lin-35* and *xnp-1* function redundantly in *C. elegans* to control the execution of lineages required for proper development of the somatic gonad during *C. elegans* postembryonic development.

Materials and methods

Strains and maintenance

Animals were propagated at 20°C according to standard methods (Sulston and Hodgkin, 1988). Strains utilized for genetic mapping include: WY142, *xnp-1(fd2) lin-35(n745); kuEx119*, outcrossed 7X to wild-type males; KR1108, *unc-11(e47) dpy-5(e61)I; hDp8(I;f)*; WY143, *unc-11(e47) xnp-1(fd2) dpy-5(e61)*; and CB4856. Strains used for phenotypic analysis include: JK2868, *lag-2::GFP(qIs56)* (Henderson et al., 1994); *xnp-1(fd2) lin-35(n745); kuEx119; lag-2::GFP*; DG1575, *lim-7::GFP* (Hall et al., 1999); *xnp-1(fd2) lin-*

35(n745); kuEx119; lim-7::GFP; MH1317, *cog-2::GFP[kuIs29]* (Hanna-Rose and Han, 1999); *dpy-5(e905) hIs29[pCeh361; pCeh363]* (Bui and Sternberg, 2002); and *xnp-1::GFP(fdEx7)*. For SynMuv genetic interactions, the following strains were used: N2; MH1461, *lin-35(n745); kuEx119* (Fay et al., 2002); *lin-9(n112); dpy-5(e61) lin-53(n833); lin-36(n766)*; and *lin-15a(n767)* (Ferguson and Horvitz, 1989).

Genetic mapping

For three-point mapping of *fd2* with *unc-11* and *dpy-5*; 15/30 Dpy non-Unc and 12/30 Unc non-Dpy retained the *xnp-1* mutation. For SNP mapping of *fd2*, CB4856 males were crossed to strain WY143 and Dpy non-Unc recombinants were isolated in subsequent generations. Because of the insensitivity of CB4856 derivatives to RNAi feeding methods, homozygous Dpy non-Unc recombinants were injected with *lin-35* double-stranded RNA, and F1 progeny were scored for the *xnp-1 lin-35* double-mutant phenotype. Using this approach, we narrowed the genomic segment containing *xnp-1(fd2)* to a small region of LGI flanked by the polymorphisms [eam60d04.s1@159,t,59] on cosmid T01A4 at position 820 and [hm42h12.s1@379,a,47] on cosmid F57C9 at position 23691. To initially identify the gene affected by the *fd2* mutation, bacterial strains containing individual RNAi-feeding clones (Fraser et al., 2000; and see RNAi section) corresponding to genes in this region were tested on *lin-35(n745)* and N2 control animals.

Other genetic methods

Tests for haploinsufficiency/semidominance were carried out by crossing *myo-2::GFP/+* males to *xnp-1(fd2)* and *xnp-1(tm678)* hermaphrodites on *lin-35(RNAi)* plates. Cross-progeny *xnp-1/+* hermaphrodites could be unambiguously identified by the presence of *myo-2::GFP*, which is expressed in the pharynx. The mating capability of *xnp-1 lin-35* mutants was assayed out by placing 15 *xnp-1 lin-35* young adult males on plates with an equal number of *dpy-11 unc-76* young adult hermaphrodites, and scoring for the appearance of non-DpyUnc cross-progeny. We failed to detect any cross-progeny on our mating plates, despite the observation that *xnp-1 lin-35* males did attempt to mate into the hermaphrodites in a manner analogous to wild-type males. To generate extrachromosomal arrays expressing the spermathecal GFP marker, *pCeh::GFP* (10 ng/μl; kindly provided by P. Sternberg and A. Rose) was coinjected with the *rol-6* marker (pRF4; 75 ng/μl) into *xnp-1, lin-35; kuEx119* hermaphrodites, and transmitting lines expressing the marker were subsequently isolated.

Transgenic rescue of *xnp-1 lin-35* mutants

Because the complete *xnp-1* gene spans two adjacent cosmids (B0041 and T04D1), a contiguous sequence for

rescue was obtained by amplifying and fusing two PCR-generated segments of genomic DNA encompassing the unspliced *xnp-1* locus as well as 3500 bp of upstream sequence. Primers used for fragment amplification are as follows: R1 [5'-CCATCGTCTCCGAAAGGTATTGATTC-3']; F1 [5'-GACTCCCATATTGGGCGCATTGTATA-3']; F2 [5'-ACTGTAATAGATCCTTCCGATGAAT-3']; R2 [5'-GGCTAAGAAGCAAGAATCTTCGGA-3']. R1 corresponds to nucleotides 5931–5956 of cosmid T04D1; F1, 1211–1235 of cosmid T04D1; R2, 1247–1270 of T04D1; F2, 22650–22675 of B0041. The F2/R1 fragment was 4745 bp long and included 3463 bp of upstream sequence. The F1/R2 fragment was 4728 bp long and included 334 bp of sequence past the *xnp-1* stop codon. These two fragments overlapped slightly and encompass a single *Bam*HI restriction site in the fourth exon. Both fragments were purified, digested with *Bam*HI, and ligated to generate a 9500-bp product. This product was further purified and injected at approximately 100–200 ng/μl along with a *sur-5::GFP* co-injection marker into *xnp-1(fd2)*, *lin-35(n745)/unc-13* heterozygotes. Non-Unc F1 progeny were picked clonally and allowed to segregate homozygous Non-Unc (*xnp-1 lin-35; fdEx-xnp-1, sur-5::GFP+*) progeny that were dependent upon the newly created *xnp-1+* array for viability. Two independent transgenic lines were obtained that both strongly rescued the *xnp-1 lin-35* lethal phenotype.

xnp-1 reporter expression

To make an *xnp-1::GFP* transcriptional fusion construct, 3500 bp of sequence upstream of the *xnp-1* start codon was amplified and cloned in frame into vector pPD95.69, which contains a GFP/nuclear localization sequence (NLS), as well as into vector pPD95.77, which contains only a GFP cassette (both kindly provided by A. Fire). Primer promf1 [5'-AGCGTGCACCATTTTCATTGAACACAT-3'] contains a *Sal*I site at the 5-prime end. Primer promr1 [5'-ATAGGATCCAACCTCATTAGTTGACA-3'] contains a *Bam*HI site at the 5-prime end and was designed to encompass the *xnp-1* start codon and preserve the GFP reading frame. PCR was done using purified T04D1 cosmid DNA. The resulting product was digested with *Sal*I and *Bam*HI and ligated to the above vectors. Microinjections for *xnp-1::GFP* expression were carried out using between 100 and 200 ng/μl of purified plasmid DNA along with the *rol-6* marker (pRF4; Mello and Fire, 1995). Several transmitting lines for each construct were obtained, all giving very similar expression patterns. One stable line containing the GFP::NLS sequence was used to generate the images shown in Fig. 5.

RNAi

The *xnp-1* RNAi construct was made by cloning a 988-bp PCR fragment of exon 4 into the polylinker of pPD129.36 (provided by A. Fire). Primers xnpRNAif [5'-

TGAACTAGTAAACCTCGTCGGAGGAA-3'] corresponding to nucleotides 547–563 of cosmid T04D1 and xnpRNAir [5'-TGACTCGAGTTTCGAGCTATGCCACG-3'] corresponding to nucleotides 1519–1535 of T04D1 were used to amplify the fragment. The recombinant vector was transformed into HT115 *E. coli*, and RNAi feeding was carried out by standard methods (Fire et al., 1998; Timmons et al., 2001).

Phasmid neuron identification

Phasmid dye filling as an indicator for execution of the T-cell lineage was carried out as previously described (Herman and Horvitz, 1994). Adult hermaphrodites were soaked in a 0.4 mg/ml solution of fluorescein isothiocyanate (FITC) in M9 solution for 4–6 h, washed three times with M9, and transferred to NGM plates.

Results

xnp-1/slr-8 is synthetically lethal with *lin-35/Rb*

We have previously described a genetic approach for identifying novel mutations that are synthetically lethal with mutations in *lin-35*, the *C. elegans* homolog of the retinoblastoma protein (Fay et al., 2002). Our screen utilizes a strain that is homozygous for a strong loss-of-function mutation in *lin-35* (*n745*) but carries an extrachromosomal array (*kuEx119*) containing both wild-type rescuing copies of *lin-35* as well as a ubiquitously expressed GFP reporter. Because *lin-35* is not an essential gene (Lu and Horvitz, 1998), the parental strain (*lin-35; kuEx119*) segregates normal-appearing GFP+ (*lin-35; kuEx119*) and GFP– (*lin-35*) progeny. Following mutagenesis, however, strains acquiring mutations that are synthetically lethal with *lin-35* (termed Slr mutants for synthetic with *lin-35/Rb*) fail to segregate normal-appearing GFP– (*lin-35; slr*) progeny. Using this approach, we identified a mutation [*slr-8(fd2)*] that defines a locus close to the center of chromosome I. Based on the molecular identity of *slr-8* (see below), we refer to this gene as *xnp-1*.

Adult animals carrying single mutations in either *lin-35* or *xnp-1* generally display no obvious morphological defects, although both single mutants exhibit a substantial reduction in brood size as compared with the wild type (Table 1; Fay et al., 2002). *xnp-1* single mutants also show a low penetrance of embryonic and larval lethality (Table 1). In contrast to single mutants, *xnp-1 lin-35* double mutants show greatly elevated levels of embryonic lethality, and surviving adults are predominantly sterile (Table 1) with pronounced defects in gonad development (see below). In addition, *xnp-1 lin-35* double mutants are slow to develop, and adults are typically small and have a clear or mottled appearance (Figs. 1A–D). We also observed an everted vulva (Evl) phenotype in

Table 1
Viability of *xnp-1* and *lin-35* mutant derivatives

Genotype	% Sterile	Average brood size	% Larval lethality ^a	% Embryonic lethality
N2 ^b	0 ($n \geq 100$)	284 ± 18 ($n = 50$)	0 ($n \geq 100$)	0 ($n \geq 100$)
<i>xnp-1(fd2)</i>	0 ($n = 24$)	74 ± 35 ($n = 24$)	14 ($n = 196$)	8 ($n = 214$)
<i>xnp-1(tm678)</i>	10 ($n = 20$)	135 ± 77 ($n = 9$)	16 ($n = 844$)	2 ($n = 713$)
<i>lin-35(n745)</i> ^b	4 ($n = 100$)	98 ± 43 ($n = 10$)	1 ($n = 268$)	6 ($n = 382$)
<i>xnp-1(fd2), lin-35</i>	99 ($n = 100$)	ND	17 ($n = 42$)	43 ($n = 106$)
<i>xnp-1(fd2)/+, lin-35</i> ^c	0 ($n = 17$)	16 ± 16 ($n = 17$)	ND	ND

^a Animals either died as larvae or failed to reach maturity after 7 days at 20°C.

^b Fay et al. (2002).

^c Heterozygous animals were generated by crossing *lin-35* males to *xnp-1, dpy-5, lin-35; kuEx119* hermaphrodites. Non-Dpy cross-progeny lacking the extrachromosomal array *kuEx119* were identified and cloned to individual plates for analysis.

approximately 50% of *xnp-1 lin-35* adults (Figs. 2C, D; also see below). Similar results were obtained by reducing *lin-35* activity in *xnp-1* single mutants by RNAi feeding methods (Figs. 1A, B; Table 2; also see below).

Animals that were homozygous for the *lin-35* mutation but heterozygous for *xnp-1(fd2)* had markedly reduced brood sizes as compared with *lin-35* single mutants (Table 1). This finding could indicate that the *xnp-1(fd2)* mutation is partially dominant or may be due to a haploinsufficiency effect. Based on additional evidence (presented below), we believe this effect is most likely due to a combination of haploinsufficiency as well as a semidominance of the *xnp-1(fd2)* allele.

xnp-1 encodes a homolog of the human disease gene, *ATR-X*

fd2 was mapped to a small region on chromosome I using a combination of genetic markers and single-nucleotide polymorphisms (SNPs; see Materials and methods). RNAi inactivation of one of the genes in the region, B0041.7 (*xnp-1*), produced no obvious phenotype in wild-type animals, but in the *lin-35* mutant background was able to replicate many aspects of the *xnp-1(fd2), lin-35* double-mutant phenotype (Table 2 and data not shown). Expression of the wild-type *xnp-1* gene product from an extrachromosomal array was able to rescue fully the lethality of *xnp-1(fd2), lin-35* double mutants (see Materials and methods),

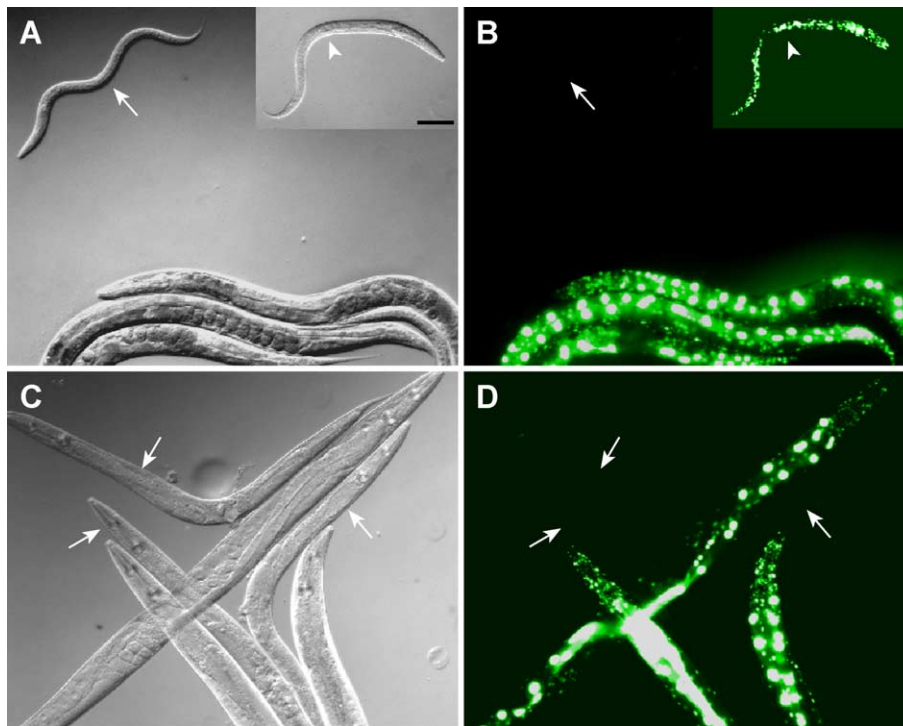


Fig. 1. Synergism between mutations in *lin-35* and *xnp-1*. DIC (A, C) and corresponding GFP fluorescence (B, D) images. The large adults with GFP fluorescence are of genotype *xnp-1 lin-35; kuEx119*. The white arrows indicate the positions of *xnp-1 lin-35* double mutants that failed to inherit the *kuEx119* extrachromosomal array. The animals in A are of the same chronological age (approximately 4 days), indicating that *xnp-1 lin-35* double mutants are slow to develop. Animals shown in C are all adults. Note the smaller size of *xnp-1 lin-35* mutant adults in C, as compared with siblings that inherited the *kuEx119*-rescuing array. Inset in A shows an *xnp-1 lin-35; kuEx119* animal in which *lin-35* was inactivated by RNAi feeding (same animal is shown in the inset in B), thus rendering the rescuing *kuEx119* array ineffective. Scale bar in A, 100 μm for A–D.

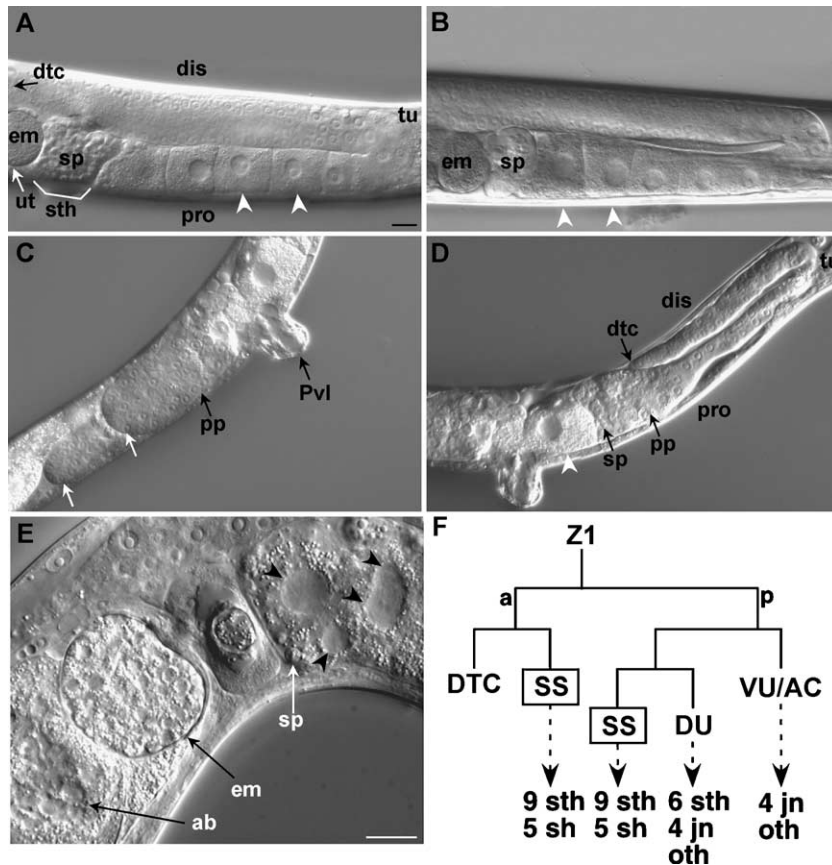


Fig. 2. DIC images of wild-type and *xnp-1 lin-35* mutant gonads. Adult wild-type (A), *xnp-1* single mutant (B), and *xnp-1 lin-35* double-mutant (C–E) gonads. Abbreviations are as follows: ab, abnormal; dis, distal gonad; dtc, distal tip cell; em, embryo; oocyte; pp, proximal germ cell proliferation; pro, proximal gonad; Pvl; protruding vulva; sh, sheath cells; sp, sperm; sth, spermatheca; tu, turn region; ut, uterus. White arrowheads in A and B designate maturing oocytes. Note the identical appearance of the gonads in panels A and B, vs. the abnormal gonadal structures displayed in panels C–E. The distal tip cell in A is located approximately 20 μm beyond the left boundary of the panel. The gonads in panels C and D are derived from the same animal (anterior and posterior, respectively). Note the clear absence of normal gonad morphology in C, as well as the diminutive size and proximal proliferation defect seen in the gonad arm in D. In addition, sperm are visible in only one of the gonad arms (D) and this animal contains only a single oocyte (C, D). Black arrowheads in E indicate what appear to be extra nuclei or abnormal cytoplasmic deposits. In addition, note the presence of the small rounded embryo (em) that has failed to undergo morphogenesis, as well as what appears to be an oocyte with abnormal nuclear morphology (ab). (F) The normal anterior somatic gonad lineage. Abbreviations are as follows: a, anterior daughter (always to left); p, posterior daughter (always to right); DU, dorsal uterine precursor; jn, spermatheca/uterine junctional cells; oth, other cell types; SS, sheath/spermathecal precursor; VU, ventral uterine precursor. The posterior gonad (derived from Z4) and the anterior gonad (derived from Z1) execute lineages with a 2-fold rotational symmetry. For additional information, see text. Scale bar in A, 10 μm for A–D; in E, 10 μm for E.

consistent with *xnp-1* being the affected gene in our mutants.

xnp-1 encodes the *C. elegans* homolog of the human ATR-X/XNP gene, a member of the Swi2/Snf2 family of ATP-dependent DEAD/DEAH box helicases (Picketts et al., 1996; reviewed by Gibbons and Higgs, 2000; Tsukiyama, 2002; Varga-Weisz, 2001). *C. elegans* XNP-1 is 34% identical and 52% similar to the human ATR-X protein over a region of 1359 amino acids (Villard et al., 1999). As discussed in the Introduction, SWI/SNF family proteins regulate transcription through localized changes in nucleosome positioning, and mutations in the human ATR-X gene lead to severe mental retardation and defects in gonad development (reviewed by Gibbons and Higgs, 2000). We sequenced the entire coding region of *xnp-1*, including the splice junction sites, and identified a single missense mutation (G \rightarrow A) at nucleotide position 3389 of the cDNA. This mutation causes an arginine to lysine sub-

stitution at position 1130 in the C terminus of the peptide. Although this substitution is relatively conservative, the normal arginine at this position is completely conserved in humans, mice, *Drosophila*, and *C. elegans*. The mutation occurs in a region of the protein that falls between the large central helicase domain (amino acids 491–1086) and the P- and Q-boxes at the far C terminus of the protein.

Through the Japanese National Bioresource Project for the Experimental Animal Nematode (Gengyo-Ando and Mitani, 2000), we also obtained a deletion allele of *xnp-1* (*tm678*). The 674-bp deletion (plus 1-bp insertion) removes amino acids 187–389 and creates a frame shift after amino acid position 186. Consistent with the results obtained for the *fd2* allele, *xnp-1(tm678)* single mutants are viable (Table 1) but the mutation is synthetically lethal in combination with *lin-35(RNAi)* (see below). RNAi feeding of *lin-35* in *xnp-1(fd2)* and *xnp-1(tm678)* single mutants resulted in similar levels of gonad morphogenesis defects: 73% ($n =$

Table 2
SynMuv Genetic interactions with *xnp-1*

Genotype	% Sterility	Average brood size	% Gonad defects
N2	<1 ($n \geq 100$)	264 ± 18 ($n = 50$)	0 ($n = 12$)
<i>(xnp-1 RNAi)</i>	0 ($n = 10$)	138 ± 38 ($n = 10$)	9 ($n = 23$)
<i>lin-35(n745)</i>	4 ($n = 100$)	98 ± 43 ($n = 10$)	10 ($n = 20$)
<i>(xnp-1 RNAi)</i>	57 ($n = 30$)	8 ± 8 ($n = 13$)	64 ($n = 45$)
<i>lin-9(n112)</i>	0 ($n = 20$)	97 ± 42 ($n = 10$)	12 ($n = 17$)
<i>(xnp-1 RNAi)</i>	20 ($n = 10$)	8 ± 10 ($n = 8$)	66 ($n = 44$)
<i>lin-36(n766)</i>	ND	115 ± 40 ($n = 10$)	5 ($n = 20$)
<i>(xnp-1 RNAi)</i>	0 ($n = 10$)	111 ± 33 ($n = 10$)	34 ($n = 47$)
<i>lin-37(n758)</i>	5 ($n = 20$)	86 ± 27 ($n = 9$)	0 ($n = 19$)
<i>(xnp-1 RNAi)</i>	10 ($n = 10$)	27 ± 25 ($n = 10$)	45 ($n = 49$)
<i>lin-53(n833)</i>	ND	86 ± 19 ($n = 10$)	0 ($n = 18$)
<i>(xnp-1 RNAi)</i>	0 ($n = 10$)	76 ± 33 ($n = 10$)	6 ($n = 11$)
<i>lin-15a(n767)</i>	ND	116 ± 29 ($n = 10$)	0 ($n = 16$)
<i>(xnp-1 RNAi)</i>	0 ($n = 10$)	120 ± 34 ($n = 10$)	4 ($n = 6$)

L4 hermaphrodites of the indicated genotypes were cloned to either control or *xnp-1(RNAi)* feeding plates and progeny were scored in the first generation. For further details, see Materials and methods.

30) of *xnp-1(fd2)* and 70% ($n = 33$) of *xnp-1(tm678)* mutants showed gonad morphogenesis defects that were very similar to those observed in *xnp-1 lin-35* double mutants. Failure of the two alleles to complement one another was indicated by the high percentage of gonad defects in *xnp-1(fd2)/xnp-1(tm678)* heterozygous animals that were treated with *lin-35(RNAi)* (by feeding methods; 78%, $n = 41$). We also compared the effects of *lin-35* inactivation (by RNAi feeding) in *xnp-1(fd2)/+* and *xnp-1(tm678)/+* heterozygous animals and observed a high percentage of gonad morphogenesis defects in both heterozygous backgrounds: 77% of *xnp-1(fd2)/+; lin-35(RNAi)* ($n = 26$) and 56% of *xnp-1(tm678)/+; lin-35(RNAi)* ($n = 32$) hermaphrodites showed gonad morphogenesis defects. These results implicate haploinsufficiency of *xnp-1* as a major cause of the defects observed in *xnp-1/+; lin-35(RNAi)* animals, since the *xnp-1* deletion allele (*tm678*) would not be expected to retain any activity. However, the observation that *xnp-1(fd2)/+; lin-35(RNAi)* animals showed a higher percentage of gonadal defects than *xnp-1(tm678)/+; lin-35(RNAi)* animals (as well as more severe morphogenesis defects; data not shown) indicates that *xnp-1(fd2)* can act semidominantly.

Although we observed the *fd2* and *tm678* alleles of *xnp-1* to be similar with respect to synthetic gonad defects, they differ with respect to other defects; *tm678* and other strong loss-of-function (LOF) alleles of *xnp-1* (but not *fd2*) show deficits in neuronal development as single mutants (Yishi Jin, personal communication). These results suggest that *xnp-1(fd2)* retains some activity, at least with respect to neuronal functions.

The structure of wild-type gonads

To understand the basis for sterility in *xnp-1 lin-35* mutants, we compared gonad development in double mutants to that of wild-type animals (for detailed descrip-

tions of wild-type gonad anatomy and development, see Hall et al., 1999; Hubbard and Greenstein, 2000; Kimble and Hirsh, 1979; Schedl, 1997). Wild-type hermaphrodites contain two symmetrical gonad arms, each of which terminates at its proximal end in the central uterine cavity. The gonad arms are roughly cylindrical in shape and take a 180° turn at their midpoints, thus marking the boundary between the proximal and distal regions (Fig. 2A). Each gonad arm is enclosed by a basement membrane and is surrounded by 10 sheath cells. The sheath cells promote germ cell proliferation and aid in mechanical aspects of ovulation (Hall et al., 1999; McCarter et al., 1997; Rose et al., 1997). In addition, sheath cells (acting through CEH-18) negatively regulate oocyte meiotic maturation (Miller et al., 2003). The distal portion of each gonad arm contains many small closely packed germ cell nuclei, whereas the proximal half houses the larger and more distantly spaced developing oocytes. The spermatheca, a structure that stores sperm cells produced during the fourth larval stage, separates the most proximal oocyte from the uterus. During ovulation, a dilation in the distal constriction of the spermatheca allows for oocytes to enter, where they become fertilized, and are deposited in the uterus.

Germ cell maturation begins in the most distal portion of the gonad, where a domain of mitotically proliferating germ cell progenitors is maintained through signals provided by the distal tip cell (DTC). Moving proximally, germ cells exit mitosis and enter into meiotic prophase in preparation for meiosis I. The stages of meiotic prophase can be visualized by DAPI staining, with each phase having a characteristic nuclear morphology (Fig. 3A; reviewed by Albertson et al., 1997; Schedl, 1997). Moving in a proximal direction from the distal-most proliferating mitotic cells, one can readily observe a transition zone, followed by regions containing pachytene, diplotene, and diakinesis-stage nuclei. The pachytene zone normally occupies about half of the distal gonad, up to the turn region. Growing oocytes with diplotene and diakinesis morphologies occupy the remainder of the (proximal) gonad, to the spermatheca.

The structure of *xnp-1 lin-35* double-mutant gonads

In comparison with wild-type animals, the gonad arms of *xnp-1 lin-35* mutants are short, narrow, and contain markedly fewer germ cells than wild-type gonads (the Glp phenotype; Figs. 2A, C, D). Using DAPI staining, we scored wild-type mid-stage adult hermaphrodites as containing on average 604 ± 141 (range 493–849, $n = 5$) germ cells in the oocyte lineage and 143 ± 24 (range 123–181, $n = 5$) in the sperm cell lineage, per gonad arm. In contrast, similarly staged *xnp-1 lin-35* double mutants contained only 140 ± 37 (range 84–191, $n = 10$) germ cells in the oocyte lineage and 21 ± 13 (range 0–41, $n = 10$) in the sperm cell lineage per gonad arm. In addition to an overall diminution in size and germ cell number, the structure of many *xnp-1 lin-35* gonads was highly abnormal; 36% ($n = 50$) of gonad

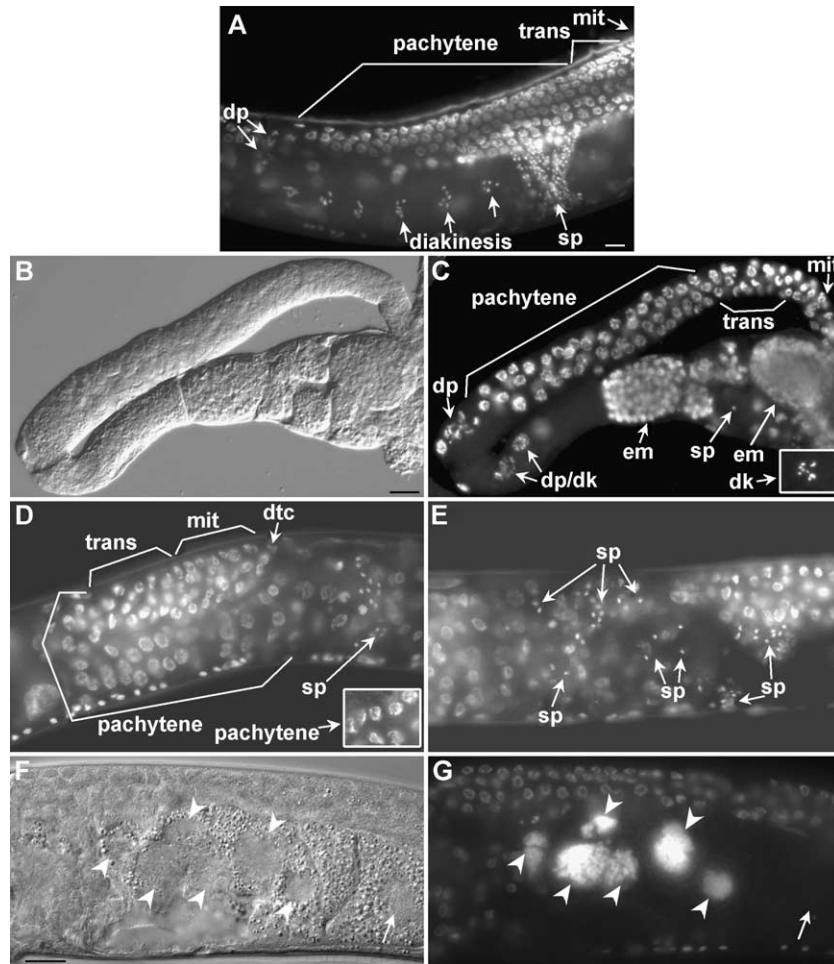


Fig. 3. DAPI staining of wild-type and *xnp-1 lin-35* mutant gonads. Adult wild-type (A) and *xnp-1 lin-35* double-mutant (B–G) gonads. B and C show corresponding DIC and DAPI images of an extruded gonad. Gonads in A, D, E, F, and G were not extruded, and other (non-germ) cell types are visible, such as ventral cord neurons. Abbreviations are as follows: dk, diakinesis; dp, diplotene; em, embryo; mit, mitotic; sp, sperm; trans, transition. The inset in C shows a diakinesis-stage oocyte obtained from an independent *xnp-1 lin-35* double-mutant animal. The inset in D shows wild-type pachytene-stage nuclei for comparison. F and G show corresponding DIC and DAPI images. White arrowheads indicate nuclei of endomitotic oocytes; the single white arrow shows a non-endomitotic oocyte. Scale bar in A, 10 μm for A; in B, 10 μm for B–E; in F, 10 μm for F and G.

arms failed to elongate properly, leading to a balled-up appearance (Fig. 2D). Even in gonad arms that were “fully” extended, an irregular morphology was often observed (Fig. 2C). In contrast to the double mutants, the large majority of *lin-35* and *xnp-1* single mutants had normal-appearing gonads (Fig. 2B; Table 2; and data not shown).

Using DIC microscopy, we observed oocytes in only 31/50 double-mutant gonad arms. Likewise, sperm were observed in only 16/38 mutant gonads (Figs. 2C, D). Moreover, when present, sperm and oocytes were substantially reduced in number and, in some cases, oocytes were observed to contain what appeared to be either multiple nuclei or cytoplasmic deposits (Figs. 2C–E). Consistent with these findings, embryos were present in only 3/25 animals (Fig. 2E), and these rare embryos were often undersized and invariably failed to undergo morphogenesis or produce viable L1 progeny. These embryos may be similar to those previously described by Rose et al. (1997), which result from defective ovulation and the subsequent

fertilization of oocyte fragments. We also observed increased numbers of small tightly packed germ cell nuclei in the proximal regions of double-mutant gonads, including those with relatively normal morphologies (Figs. 2C, D). Finally, most mutant animals displayed an Evi phenotype (Figs. 2C, D), which could reflect developmental defects in either the vulva or proximal somatic gonad. However, as we found no evidence for vulval induction or lineage defects in the double mutants (data not shown), this phenotype is likely due to developmental defects in the somatic gonad.

We also examined *xnp-1 lin-35* males for gonad morphogenesis defects as well as the ability to mate. While all of the double-mutant males examined displayed subtle differences from the wild type ($n = 9$), only five showed obvious morphogenetic defects, and these were in general less severe than the defects observed in *xnp-1 lin-35* hermaphrodites (data not shown). In addition, 9/9 *xnp-1 lin-35* males contained sperm and possessed a normal appearing mating apparatus in the tail (data not shown). In addition, *xnp-1 lin-*

35 males displayed stereotypical mating behaviors in the presence of hermaphrodites. Nevertheless, *xnp-1 lin-35* males were completely defective at mating (see Materials and methods), suggesting that *xnp-1 lin-35* males may have subtle defects in the structure and/or function of the male gonad/mating apparatus.

Germ cell maturation in xnp-1 lin-35 double mutants

We used DAPI staining to follow germ cell development in *xnp-1 lin-35* mutant hermaphrodites. Based on nuclear morphologies, germ cell progression in the distal half of the gonad appeared to proceed normally in gonad arms that had undergone complete extension ($n = 37$). We consistently observed a proliferation zone in the most distal portion of the gonad, followed by nuclei with typical transition and pachytene morphologies (Figs. 3B, C). However, the area occupied by pachytene-stage cells in many cases extended well into the proximal gonad region, where oocytes would normally be located (24/37 gonad arms were defective at pachytene exit; Fig. 3D). The relatively normal appearance of the distal gonad is consistent with our finding that double-mutant gonads typically contain a single DTC (39/40, based on a *lag-2::GFP* reporter; Henderson et al., 1994), which is required for maintenance of a proliferation zone and for indirectly controlling the onset of meiosis.

Forming oocytes with recognizable diplotene and diakinesis-stage nuclear morphologies were detectable in about half (21/50) of the double-mutant gonads (Figs. 3B–E). In addition, we observed endomitotic oocytes (the Emo phenotype), in which abnormal DNA replication cycles produce highly polyploid oocytes, in 50% ($n = 32$) of the double-mutant gonads (Figs. 3F, G). This defect has been associated with a failure of oocytes to be fertilized in a timely manner following maturation (Greenstein et al., 1994; Iwasaki et al., 1996; Myers et al., 1996; Ward and Carrel, 1979). Small abnormal-appearing embryos were also observed in approximately 20% of mutant gonads (Figs. 3B, C; also see above). We also observed sperm cell nuclei by DAPI staining in 29/30 double-mutant animals. However, the number of sperm cells was dramatically reduced as compared with wild-type animals (Figs. 3C–E; also see above). In addition, sperm cells were typically present in ectopic locations, such as in the region of the uterus (Fig. 3E). This contrasts with wild-type animals, where sperm cells are consistently concentrated in the spermatheca (Figs. 2A, 3A).

xnp-1 lin-35 mutants are defective at sheath and spermathecal cell development

The phenotypes described above are strikingly similar to those previously reported in a detailed study by McCarter et al. (1997) on the effects of somatic gonad cell ablations. Specifically, ablation of both sheath/spermathecal (SS) precursor cells at the L2/L3 molt produced gonads of diminutive size and a reduced number of germ cells, which

were defective at pachytene exit. Furthermore, ablation of single SS cells at this stage led to the appearance of endomitotic oocytes and in many cases, an absence or reduction in the number of sperm cells (the Fog phenotype). Given that we had observed the same spectrum of defects in *xnp-1 lin-35* double mutants, it seemed likely that *xnp-1 lin-35* mutants are defective in the execution of the SS lineage, leading to reduced numbers of sheath and spermathecal cells. To test directly for effects on the sheath cell development, we made use of the *lim-7::GFP* reporter (Hall et al., 1999), which is expressed consistently in the cytoplasm (and more variably in the nuclei) of eight of the ten sheath cells (pairs 1–4) surrounding each gonad arm (Figs. 4A, B). Strikingly, 42% ($n = 38$) of gonad arms from *xnp-1 lin-35* mutants failed to show any detectable *lim-7::GFP* expression, indicating that at least eight of the ten sheath cells are missing in these gonads (Figs. 4C, D). Absence of GFP expression was observed both for gonad arms with highly irregular morphologies (Fig. 4D) as well as some displaying relatively normal morphologies (data not shown). Moreover, among the mutant gonad arms that expressed the marker, we saw on average a 3- to 4-fold reduction in the number of GFP-positive sheath cell nuclei as compared with the wild type [1.1 ± 1.3 ; range 1–4 ($n = 16$) in *xnp-1 lin-35* mutants vs. 4.8 ± 1.3 ; range 2–8 ($n = 30$) for the wild type]. These findings indicate that sheath cell production, differentiation, and/or survival is greatly compromised in *xnp-1 lin-35* mutants. However, it remains possible that sheath cells are generated but fail to express the *lim-7::GFP* marker.

Our inability to detect a spermatheca, as well as the presence of ectopic sperm cells in *xnp-1 lin-35* adults, suggested that the spermathecal cell lineage or differentiation has been significantly altered in the double mutants. To further examine this, we made use of a GFP marker for spermathecal cells (*pCeh::GFP*; Figs. 4E, F; Bui and Sternberg, 2002). Because the integration site of the spermathecal marker was located on LGI at a proximal location to *lin-35* and *xnp-1*, we were unable to construct a double-mutant strain containing the integrated marker. Instead, we injected the plasmid encoding the marker (see Materials and methods) into *xnp-1 lin-35; kuEx119* hermaphrodites and obtained several lines that carried both the spermathecal marker (e.g., *fdEx10*) and *lin-35 (kuEx119)* on a separate extrachromosomal arrays. In double-mutant animals containing both arrays, we detected expression of the spermathecal marker in 21/21 animals, whereas spermathecal GFP was only observed in 12/25 *xnp-1 lin-35* double mutants that failed to segregate the *lin-35*-rescuing array (*kuEx119*; Figs. 4G, H). Furthermore, while animals with both arrays generally showed bilateral expression of the spermathecal marker (15/21), *kuEx119*-minus animals rarely displayed bilateral expression of the marker (2/25). Taken together, *xnp-1 lin-35* mutants appear to be defective in the generation, differentiation, or survival of both cell types that are derived from the SS precursors.

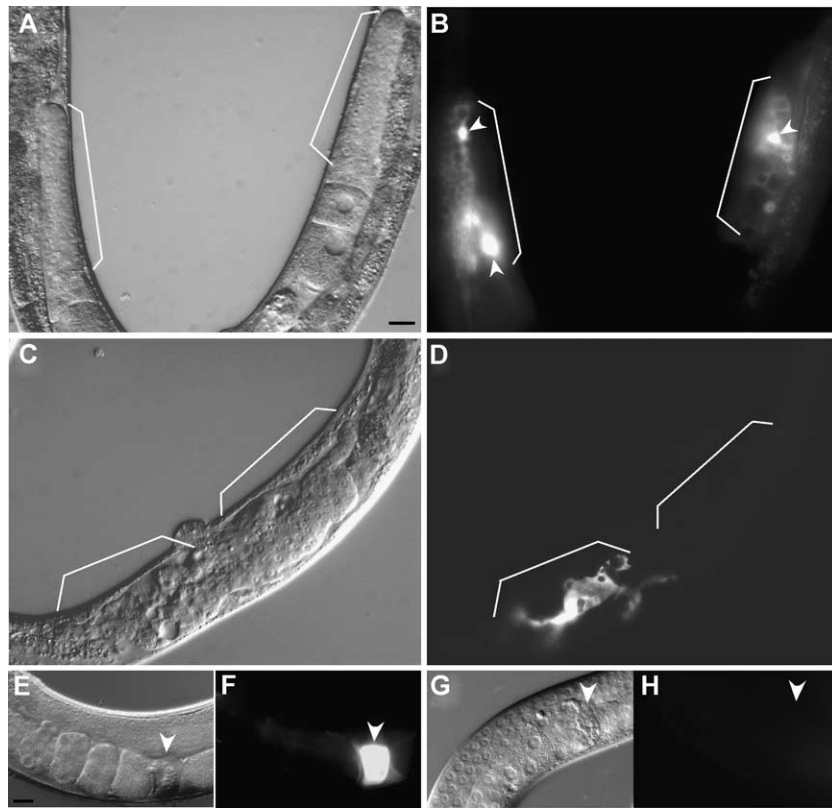


Fig. 4. Marker expression in sheath and spermatheca cells in wild-type and *xnp-1 lin-35* mutant gonads. Corresponding DIC (A, C, E, G) and GFP (B, D, F, H) images of wild-type (A, B, E, F) and *xnp-1 lin-35* double-mutant (C, D, G, H) adult hermaphrodites. *lim-7::GFP* is normally expressed in the cytoplasm of eight of the ten sheath cells (pairs 1–4) surrounding each gonad arm. In addition, more variable expression can be seen in the nuclei of sheath cells (white arrowheads; also see text). White brackets indicate the expected locations of sheath cell pairs 1–4. Note the complete absence of expression in one of the *xnp-1 lin-35* mutant gonad arms (panels C, D; right bracket), whereas expression in the opposite arm appears reduced, disorganized, and proximally displaced compared to the wild type. E–G show expression of the spermathecal marker pCeh::GFP. White arrowheads indicate the location of sperm. Note the complete absence of marker expression in the mutant gonad arm (H). Scale bars for panel A, 10 μ m for A–D; in E, 10 μ m for E–H.

As discussed above, we observed normal expression of the DTC marker (using *lag-2::GFP*) in 39/40 gonad arms of double-mutant adults, including those that had failed to undergo appreciable extension. It also appeared from the normal pattern of vulval cell induction that an anchor cell (AC) is also reliably generated in double-mutant animals. This latter observation suggested that the DTC and possibly AC/VU lineages are less affected in the double mutants than is the SS lineage (Fig. 2F). To further examine effects on the VU lineage, we made use of the *cog-2::GFP* marker, which is expressed in a subset of VU cells that adopt the π fate. In wild-type hermaphrodites, a total of 12 π cells are generated, which further differentiate to form the multinucleate uterine seam cell as well as uv1 cells of the ventral uterus (Newman et al., 1996). Consistent with previous reports, we always observed 12 π cells ($n = 15$) in wild-type hermaphrodites by the mid-L4 stage (Hanna-Rose and Han, 1999). In *xnp-1 lin-35* mutants, we detected an average of 14.4 ± 2.4 (range 12–18, $n = 11$) π cells at the mid-L4 stage. This result indicates that unlike the missing SS descendants, π cells of the ventral uterus are reliably generated. The slightly increased numbers of π cells in *xnp-1 lin-35* mutants could

be due to extra divisions of the π cells, an increased produrance of the GFP marker in π -cell sister lineages (such as the ρ cells), or possibly an alteration in the fates of some SS derivatives to the π -cell fate. Taken together, these findings indicate that the many gonadal deficits observed in the double mutants can be largely attributed to defects in the generation or specification of sheath and spermathecal cells (the SS lineage).

xnp-1 mutants show weak defects in T-cell differentiation and alae formation

Previous studies implicated two SWI/SNF complex components (*psa-1* and *psa-4*) in the control of the *C. elegans* T cell lineage (Sawa et al., 2000). In wild-type animals, the anterior daughter of the T cell gives rise to two hypodermal cells, whereas the posterior daughter generates two phasmid neurons and their accompanying socket cells (Sulston and Horvitz, 1977). PSA-1 and PSA-4 are most similar to yeast Swi3 and Swi2 proteins, respectively. Mutations in both genes lead to variable defects in the T cell lineage, resulting in the posterior cell adopting an anterior-like (hypodermal) fate.

The fates of T cells can be monitored through a passive dye filling assay using the compound FITC (see Materials and methods). We found that both the wild type and *lin-35* mutants always contain four T cell-derived FITC⁺ neurons/socket cells ($n = 20$ and $n = 13$, respectively), indicating that *lin-35* single mutants are not defective at T cell differentiation. In contrast, *psa-4(os13)* single mutants contained an average of 2.7 ± 1.0 ($n = 20$; range 1–4) T cell-derived FITC⁺ cells. *xnp-1(fd2)* and *xnp-1(tm678)* single mutants also showed reduced numbers of T cell-derived neurons: 3.3 ± 0.9 ($n = 19$; range 1–4) and 3.6 ± 1.0 ($n = 18$; range 0–4), respectively. The effect was, however, markedly less pronounced than that observed for *psa-4* mutants. Interestingly, the presence of the *lin-35* mutation in the *xnp-1(fd2)* mutant background did not enhance the T cell lineage defect (3.5 ± 0.9 , $n = 17$, range 1–4), indicating that *xnp-1* functions non-redundantly with *lin-35* in T cell differentiation.

To look for additional defects in non-gonadal lineages during postembryonic development, we examined *xnp-1 lin-35* double mutants for defects in the formation of alae. Alae are observed as striations along the lateral cuticle and are produced in adult animals by the left and right seam cell syncytiums. We observed short interruptions in the normal alae pattern in 5/10 *xnp-1, lin-35* adult hermaphrodites, suggesting a possible underlying defect in the generation or fusion of the hypodermal seam cells in some of the mutants. Interestingly, defects in alae were generally not observed in male double-mutant animals (1/9). The decreased penetrance of both the alae and gonadal defects in males relative to double-mutant hermaphrodites suggests that males may somehow be better able to compensate for the loss of *xnp-1* and *lin-35* than hermaphrodites.

xnp-1::GFP reporter analysis

To determine the expression pattern of *xnp-1* during development, we generated GFP transcriptional reporter constructs containing approximately 3500 bp of *xnp-1* upstream regulatory sequences. Importantly, the upstream promoter region used in the reporter constructs was identical to that used for the successful *xnp-1* rescue experiments. *xnp-1::GFP* is expressed in most cells during embryonic development, beginning at around the 100- to 200-cell stage of embryogenesis (Figs. 5A–D). Interestingly, *xnp-1::GFP* expression was reproducibly absent or greatly reduced in the intestinal cell lineages, suggesting that *xnp-1* expression is not ubiquitous (Figs. 5A–D). Strong expression of *xnp-1::GFP* becomes restricted during late stages of embryogenesis, with highest levels of expression occurring in neuronal cells of the head, ventral nerve cord, and tail.

During larval development, *xnp-1::GFP* is expressed predominantly in neurons (Figs. 5E–H). However, strong expression was reproducibly observed in the junctional cells of the spermatheca and uterus (Figs. 5E, F). In addition, we detected variable and weaker expression in other cells of the somatic gonad, such as the DTC, and in what appeared to be

the thin outline of sheath cells surrounding the gonad (Figs. 5E, F). A lack of robust reporter expression in spermathecal and sheath cells could indicate that the effect of *xnp-1* mutations on the SS lineage may be indirect. However, it is also possible that *xnp-1* acts autonomously in these cells but at levels that are below the detection of our reporter constructs. Consistent with this, other SWI/SNF components are known to function at levels in the range of approximately 200 molecules per cell (Cairns et al., 1996; Cote et al., 1994). Finally, although active transcription of *xnp-1* may abate in cells of the SS lineage during larval stages of development, significant levels of XNP-1 protein may be retained from earlier stages or be produced through the translation of mRNAs generated earlier in development.

xnp-1 is synthetically lethal with other class B SynMuv genes

lin-35 was originally identified as a member of the SynMuv gene family (Ferguson and Horvitz, 1989; Lu and Horvitz, 1998). Strains carrying mutations in both *lin-35*, a class B SynMuv gene, and class A SynMuv genes such as *lin-15a* lead to a highly penetrant multivulval (Muv) phenotype (Ferguson and Horvitz, 1989; reviewed by Fay and Han, 2000). Given that *lin-35* is a member of the class B synMuv gene family, we were interested to determine whether *xnp-1* showed synthetic genetic interactions with other members of the SynMuv gene family. Of the four class B SynMuv genes tested, three showed significant increases in the percentage of adults with gonad defects (*lin-9, lin-36, lin-37*) whereas *lin-53/RbAP* failed to show any effects (Table 2). Interestingly, strong LOF alleles of *lin-9*, a gene with homology to *Drosophila* Aly (a protein associated with chromatin; White-Cooper et al., 2000), have also been reported to cause defects in sheath cell development (Beitel et al., 2000). We also tested *lin-15a*, a member of the class A SynMuv gene family, but failed to observe any synthetic interaction (Table 2). The incomplete penetrance of the gonad phenotypes, including those displayed by *lin-35; xnp-1(RNAi)* adults (Table 2), may be due to deficiencies in the RNAi method for gene inactivation. Alternatively, partial penetrance may also reflect an incomplete requirement for the gene in the regulation of gonad morphogenesis with *xnp-1*. From these experiments, we conclude that at least a subset of other class B members can genetically interact with mutations in *xnp-1*.

Discussion

Multiple classes of lin-35 synthetic mutations

We have reported on the cloning and characterization of three mutations, each of which leads to distinct synthetic phenotypes in conjunction with *lin-35/Rb* LOF. The first class, defined by *fzr-1*, led to abnormal cell cycle reentry

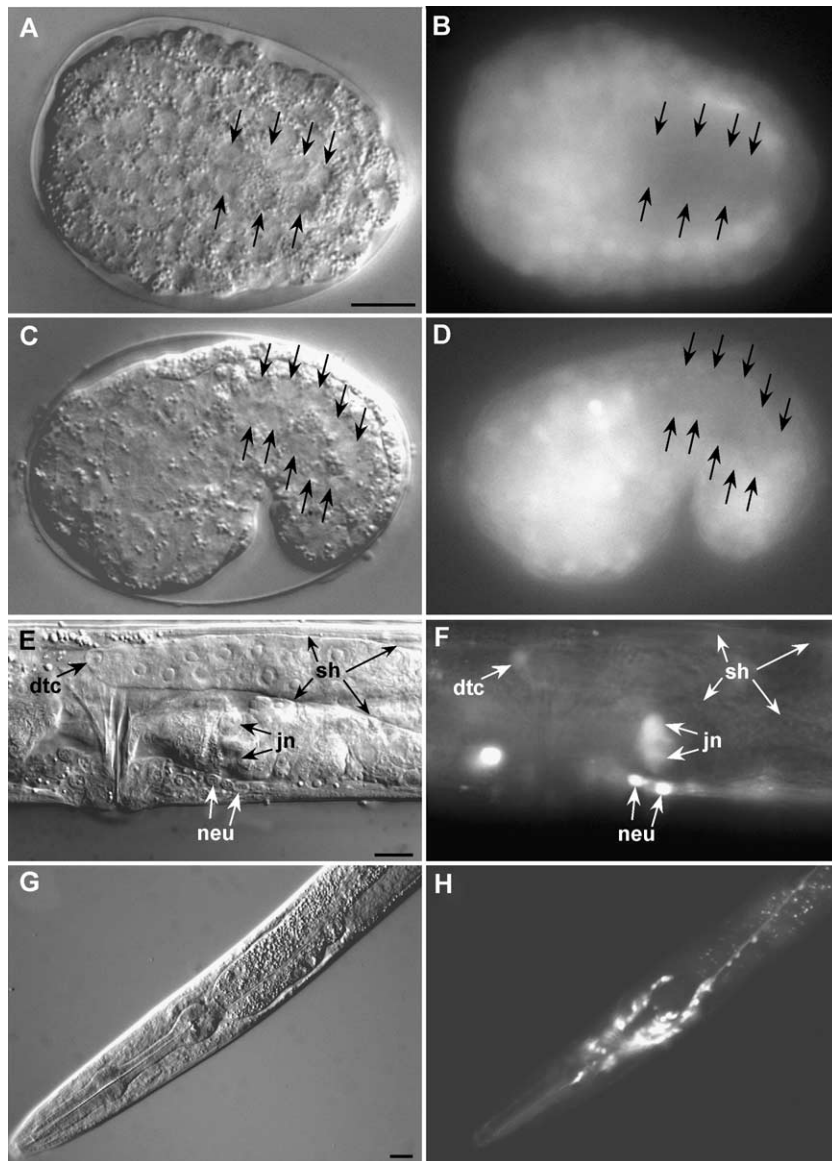


Fig. 5. *xnp-1::GFP* reporter expression. Corresponding DIC (A, C, E, G) and GFP fluorescence (B, D, F, H) images of *xnp-1::GFP* reporter expression in wild-type animals. Arrows in A–D indicate the approximate positions of intestinal cell nuclei in bean- (A, B) and comma-bean- (C, D) stage embryos. Note the reduced GFP expression in these cells relative to other cell types. E and F show expression in the gonad region of an adult hermaphrodite. Abbreviations are as follows: dtc, distal tip cell; jn, spermatheca/uterine junctional cells; neu, neuronal cells of the ventral nerve cord; sh, sheath cell. G and H show GFP expression in head neurons in an L3 larva. Scale bars for panel A, 10 μ m for A–D; in E, 10 μ m for E, F; in G, 10 μ m for G, H.

and excess proliferation in most postembryonic blast lineages (Fay et al., 2002). The second class, defined by *ubc-18*, caused no obvious defects in proliferation or differentiation but instead affected an early step of pharyngeal morphogenesis during embryonic development (Fay et al., 2003). *xnp-1* defines a third class of *lin-35* synthetic mutations, in which subsets of cell types appear to be missing or greatly diminished in number. Specifically, *xnp-1 lin-35* double mutants failed to properly generate sheath and spermathecal cells, two cell types that contribute to the structure of the somatic gonad and that are derived in large part from four progenitors, the SS cells (Fig. 2F).

The phenotype of *xnp-1 lin-35* double mutants also differs markedly from that of the SynMuv mutants. In wild-

type hermaphrodites, an inductive signal from the gonadal anchor cell normally triggers Ras/Map kinase pathway activation in three of the six vulval precursor cells, causing them to adopt a vulval cell fate (reviewed by Greenwald, 1997). However, in hermaphrodites carrying SynMuv mutations, the acquisition of vulval cell fates is no longer dependent on Ras/Map kinase pathway signaling (reviewed by Fay and Han, 2000). This independence from Ras/Map kinase signaling leads to the adoption of vulval cell fates by all six of the precursor cells, including three that would normally have acquired hypodermal identities. This circumstance of combining independence from signaling and cell fate transformations differs significantly from that of *xnp-1 lin-35* mutants in two respects. (1) There is currently no

evidence to suggest that signaling is required to induce the SS cell fate or that of its sister lineages (DTC and DU). (2) We obtained no data to indicate that cell types that are connected by lineage to SS cells (see Fig. 2F), such as the DTC, are being overproduced (see Results). Thus, *xnp-1* defines a fourth generic class of *lin-35* synthetic mutation whereby specific lineages or developmental programs fail to be executed.

It is interesting to note that of the four classes of *lin-35* synthetic mutations thus far described, only one, that defined by *fzr-1*, appears to be connected to cell cycle regulation. This statement is based on both detailed analyses of the mutant phenotypes as well as the observed genetic interactions of *xnp-1*, *ubc-18*, and class A SynMuv genes with certain class B SynMuv members, such as *lin-37*, that do not appear to function in cell cycle control (Boxem and van den Heuvel, 2002; Fay et al., 2003; Ferguson and Horvitz, 1989; Table 2). These genetic data lend further credence to the view that the phenotypes observed for many of the *lin-35* synthetic mutants are unconnected to cell cycle defects and that *lin-35* carries out multiple functions that are independent of its canonical role as a cell cycle regulator.

Synergism between lin-35 and a chromatin-remodeling enzyme

xnp-1 encodes the *C. elegans* homolog of the human ATR-X gene, a member of the Swi/Snf superfamily of ATP-dependent chromatin remodeling helicases (Picketts et al., 1996; Villard et al., 1999). Mutations in human ATR-X lead to severe mental retardation as well as many secondary anomalies including urogenital defects in approximately 80% of ATR-X patients (reviewed by Gibbons and Higgs, 2000). The mutation identified in *xnp-1(fd2)* mutants leads to a substitution (R → K) of a highly conserved arginine at amino acid position 1130 (corresponding to human ATR-X position 2197) in the C terminus of the peptide. Interestingly, an analysis of molecular lesions from ATR-X patients indicates that mutations affecting the C-terminal region of the ATR-X protein are often associated with the most severe forms of urogenital defects (Gibbons and Higgs, 2000). In contrast to humans, however, expression of the gonadal defect in *C. elegans* is dependent upon the coordinate inactivation of class B SynMuv genes such as *lin-35* (Table 2). Thus, in *C. elegans*, *lin-35* and *xnp-1* function redundantly in the control of gonadal development.

Studies on Swi/Snf family members have indicated their importance in many diverse biological processes, most of which can be linked mechanistically to the control of nucleosome remodeling and gene expression (reviewed by Havas et al., 2001; Sudarsanam and Winston, 2000; Tsukiyama, 2002; Varga-Weisz, 2001). The precise level of control exerted by Swi/Snf members has been reported to range from gene-specific to global and appears to

depend on several factors including the particular Swi/Snf complex involved, associations with various binding partners (e.g., Cosma et al., 1999; Dimova et al., 1999; Natarajan et al., 1999; Neely et al., 1999; Yudkovsky et al., 1999), genetic background (Biggar and Crabtree, 1999; Sudarsanam et al., 1999), and cell cycle phase (Berube et al., 2000; Krebs et al., 2000). Moreover, the effects exerted by Swi/Snf complexes on individual target genes can be either repressive or activating; the outcome most likely depends on the influence of other bound regulators such as histone modifying enzymes (Agalioti et al., 2000; Cosma et al., 1999; Dilworth et al., 2000; Hassan et al., 2001).

An obvious model to account for the functional redundancy of LIN-35 and XNP-1 is that both proteins share in common one or more transcriptional targets. Thus, in single-mutant backgrounds, sufficient regulation of the target can be brought about through the intact pathway acting alone. However, in double mutants, two means of regulation are missing and the shared target (or targets) may become grossly deregulated. We note that based on precedent from studies on the transcriptional effects of Rb family members (reviewed by Dyson, 1998; Harbour and Dean, 2000), as well as our own studies on other *lin-35* synthetic mutants (Fay et al., 2002, 2003; and unpublished data), we expect the actions of both LIN-35 and XNP-1 on the shared target(s) to be repressive in nature.

As to how many common targets might be affected in the double mutants is an open question. Many studies analyzing the transcriptional targets of individual Swi/Snf complexes have been carried out, and they suggest that Swi/Snf proteins may regulate the expression of sizeable numbers (on the order of several hundred to several thousand) of physically disparate target genes (e.g., Angus-Hill et al., 2001; Damelin et al., 2002; Holstege et al., 1998; Sudarsanam et al., 2000; Ng et al., 2002). Likewise, many recent reports seeking to determine the transcriptional targets of Rb family members suggest that Rb family members may collectively regulate the expression of up to several hundred genes (Black et al., 2003; Markey et al., 2002; Russo et al., 2003; Vernell et al., 2003; Wells et al., 2003). Although such studies may be significantly compromised by issues such as cell- and tissue-type specific differences, genetic redundancy, and indirect effects, they provide at least some basis for estimating the number of genes that may be co-regulated by LIN-35 and XNP-1 in *C. elegans*. Namely, assuming a nonbiased set of 250 independent targets for both LIN-35 and XNP-1, as well as a genome consisting of 17,000 genes, we would predict that on average, 3.7 genes would be regulated by both factors. Although such calculations are highly speculative, they do suggest that the observed phenotype of *xnp-1 lin-35* mutants could be due to the misexpression of a relatively small number of genes, perhaps even a single common target. Identification of such targets, either by genetics or other means, will await further studies.

Acknowledgments

We would like to thank the *C. elegans* Genetics Consortium, David Greenstein, Paul Sternberg, Judith Kimble, Paul Sternberg, Wendy Hanna-Rose, Ann Rose, and the National Biosource Project for the Experimental animal Nematode *C. elegans* for strains and constructs. We thank Amy Fluet for a critical reading of the manuscript and David Greenstein, Jane Hubbard, and Darrel Killian for helpful advice. We thank Yishi Jin and Jonathan Ewbank for communicating unpublished data. We also thank Andy Fire for expression constructs. This work was supported by a research grant from the American Cancer Society and the University of Wyoming.

References

- Agalioti, T., Lomvardas, S., Parekh, B., Yie, J., Maniatis, T., Thanos, D., 2000. Ordered recruitment of chromatin modifying and general transcription factors to the IFN-beta promoter. *Cell* 103, 667–678.
- Albertson, D.G., Rose, A.M., Villanueva A.M., 1997. Chromosomes, mitosis, and meiosis. In: Riddle, D.L., Blumenthal, T., Meyer, B.J., Priess, J.T. (Eds.), *C. elegans* II. Cold Spring Harbor Laboratory Press, Cold Spring Harbor, NY, pp. 47–78.
- Angus-Hill, M.L., Schlichter, A., Roberts, D., Erdjument-Bromage, H., Tempst, P., Cairns, B.R., 2001. A Rsc3/Rsc30 zinc cluster dimer reveals novel roles for the chromatin remodeler RSC in gene expression and cell cycle control. *Mol. Cell* 7, 741–751.
- Bazett-Jones, D.P., Cote, J., Landel, C.C., Peterson, C.L., Workman, J.L., 1999. The SWI/SNF complex creates loop domains in DNA and polynucleosome arrays and can disrupt DNA-histone contacts within these domains. *Mol. Cell. Biol.* 19, 1470–1478.
- Beitel, G.J., Lambie, E.J., Horvitz, H.R., 2000. The *C. elegans* gene lin-9, which acts in an Rb-related pathway, is required for gonadal sheath cell development and encodes a novel protein. *Gene* 254, 253–263.
- Beube, N.G., Smeenk, C.A., Picketts, D.J., 2000. Cell cycle-dependent phosphorylation of the ATRX protein correlates with changes in nuclear matrix and chromatin association. *Hum. Mol. Genet.* 9, 539–547.
- Biggar, S.R., Crabtree, G.R., 1999. Continuous and widespread roles for the Swi-Snf complex in transcription. *EMBO J.* 18, 2254–2264.
- Black, E.P., Huang, E., Dressman, H., Rempel, R., Laakso, N., Asa, S.L., Ishida, S., West, M., Nevins, J.R., 2003. Distinct gene expression phenotypes of cells lacking Rb and Rb family members. *Cancer Res.* 63, 3716–3723.
- Boxem, M., van den Heuvel, S., 2002. *C. elegans* class B synthetic multivulva genes act in G(1) regulation. *Curr. Biol.* 12, 906–911.
- Brehm, A., Miska, E.A., McCance, D.J., Reid, J.L., Bannister, A.J., Kouzarides, T., 1998. Retinoblastoma protein recruits histone deacetylase to repress transcription. *Nature* 391, 597–601.
- Bui, Y.K., Sternberg, P.W., 2002. *Caenorhabditis elegans* inositol 5-phosphatase homolog negatively regulates inositol 1,4,5-triphosphate signaling in ovulation. *Mol. Biol. Cell* 13, 1641–1651.
- Cairns, B.R., Lorch, Y., Li, Y., Zhang, M., Lacomis, L., Erdjument-Bromage, H., Tempst, P., Du, J., Laurent, B., Kornberg, R.D., 1996. RSC, an essential, abundant chromatin-remodeling complex. *Cell* 87, 1249–1260.
- Cosma, M.P., Tanaka, T., Nasmyth, K., 1999. Ordered recruitment of transcription and chromatin remodeling factors to a cell cycle- and developmentally regulated promoter. *Cell* 97, 299–311.
- Cote, J., Quinn, J., Workman, J.L., Peterson, C.L., 1994. Stimulation of GAL4 derivative binding to nucleosomal DNA by the yeast SWI/SNF complex. *Science* 265, 53–60.
- Damelin, M., Simon, I., Moy, T.I., Wilson, B., Komili, S., Tempst, P., Roth, F.P., Young, R.A., Cairns, B.R., Silver, P.A., 2002. The genome-wide localization of Rsc9, a component of the RSC chromatin-remodeling complex, changes in response to stress. *Mol. Cell* 9, 563–573.
- Dilworth, F.J., Fromental-Ramain, C., Yamamoto, K., Chambon, P., 2000. ATP-driven chromatin remodeling activity and histone acetyltransferases act sequentially during transactivation by RAR/RXR In vitro. *Mol. Cell* 6, 1049–1058.
- Dimova, D., Nackerdien, Z., Furgeson, S., Eguchi, S., Osley, M.A., 1999. A role for transcriptional repressors in targeting the yeast Swi/Snf complex. *Mol. Cell* 4, 75–83.
- Dunaief, J.L., Strober, B.E., Guha, S., Khavari, P.A., Alin, K., Luban, J., Begemann, M., Crabtree, G.R., Goff, S.P., 1994. The retinoblastoma protein and BRG1 form a complex and cooperate to induce cell cycle arrest. *Cell* 79, 119–130.
- Dyson, N., 1998. The regulation of E2F by pRB-family proteins. *Genes Dev.* 12, 2245–2262.
- Fay, D.S., Han, M., 2000. The synthetic multivulval genes of *C. elegans*: functional redundancy, Ras-antagonism, and cell fate determination. *Genesis* 26, 279–284.
- Fay, D.S., Keenan, S., Han, M., 2002. *fzr-1* and *lin-35/Rb* function redundantly to control cell proliferation in *C. elegans* as revealed by a nonbiased synthetic screen. *Genes Dev.* 16, 503–517.
- Fay, D.S., Large, E., Han, M., Darland, M., 2003. *lin-35/Rb* and *ubc-18*, an E2 ubiquitin-conjugating enzyme, function redundantly to control pharyngeal morphogenesis in *C. elegans*. *Development* 130, 3319–3330.
- Ferguson, E.L., Horvitz, H.R., 1989. The multivulva phenotype of certain *Caenorhabditis elegans* mutants results from defects in two functionally redundant pathways. *Genetics* 123, 109–121.
- Fire, A., Xu, S., Montgomery, M.K., Kostas, S.A., Driver, S.E., Mello, C.C., 1998. Potent and specific genetic interference by double-stranded RNA in *Caenorhabditis elegans*. *Nature* 391, 806–811.
- Fraser, A.G., Kamath, R.S., Zipperlen, P., Martinez-Campos, M., Sohrmann, M., Ahringer, J., 2000. Functional genomic analysis of *C. elegans* chromosome I by systematic RNA interference. *Nature* 408, 325–330.
- Gavin, I., Horn, P.J., Peterson, C.L., 2001. SWI/SNF chromatin remodeling requires changes in DNA topology. *Mol. Cell* 7, 97–104.
- Gengyo-Ando, K., Mitani, S., 2000. Characterization of mutations induced by ethyl methanesulfonate, UV, and trimethylpsoralen in the nematode *Caenorhabditis elegans*. *Biochem. Biophys. Res. Commun.* 269, 64–69.
- Gibbons, R.J., Higgs, D.R., 2000. Molecular-clinical spectrum of the ATR-X syndrome. *Am. J. Med. Genet.* 97, 204–212.
- Greenstein, D., Hird, S., Plasterk, R.H., Andachi, Y., Kohara, Y., Wang, B., Finney, M., Ruvkun, G., 1994. Targeted mutations in the *Caenorhabditis elegans* POU homeo box gene *ceh-18* cause defects in oocyte cell cycle arrest, gonad migration, and epidermal differentiation. *Genes Dev.* 8, 1935–1948.
- Greenwald, I., 1997. Development of the vulval. In: Riddle, D.L., Blumenthal, T., Meyer, B.J., Priess, J.T. (Eds.), *C. elegans* II. Cold Spring Harbor Laboratory Press, Cold Spring Harbor, NY, pp. 519–541.
- Hall, D.H., Winfrey, V.P., Blaeuer, G., Hoffman, L.H., Furuta, T., Rose, K.L., Hobert, O., Greenstein, D., 1999. Ultrastructural features of the adult hermaphrodite gonad of *Caenorhabditis elegans*: relations between the germ line and soma. *Dev. Biol.* 212, 101–123.
- Hamiche, A., Sandaltzopoulos, R., Gdula, D.A., Wu, C., 1999. ATP-dependent histone octamer sliding mediated by the chromatin remodeling complex NURF. *Cell* 97, 833–842.

- Hanna-Rose, W., Han, M., 1999. COG-2, a sox domain protein necessary for establishing a functional vulval-uterine connection in *Caenorhabditis elegans*. *Development* 126, 169–179.
- Harbour, J.W., Dean, D.C., 2000. The Rb/E2F pathway: expanding roles and emerging paradigms. *Genes Dev.* 14, 2393–2409.
- Hassan, A.H., Neely, K.E., Workman, J.L., 2001. Histone acetyltransferase complexes stabilize swi/snf binding to promoter nucleosomes. *Cell* 104, 817–827.
- Havas, K., Flaus, A., Phelan, M., Kingston, R., Wade, P.A., Lilley, D.M., Owen-Hughes, T., 2000. Generation of superhelical torsion by ATP-dependent chromatin remodeling activities. *Cell* 103, 1133–1142.
- Havas, K., Whitehouse, I., Owen-Hughes, T., 2001. ATP-dependent chromatin remodeling activities. *Cell. Mol. Life Sci.* 58, 673–682.
- Henderson, S.T., Gao, D., Lambie, E.J., Kimble, J., 1994. lag-2 may encode a signaling ligand for the GLP-1 and LIN-12 receptors of *C. elegans*. *Development* 120, 2913–2924.
- Herman, M.A., Horvitz, H.R., 1994. The *Caenorhabditis elegans* gene lin-44 controls the polarity of asymmetric cell divisions. *Development* 120, 1035–1047.
- Holstege, F.C., Jennings, E.G., Wyrick, J.J., Lee, T.I., Hengartner, C.J., Green, M.R., Golub, T.R., Lander, E.S., Young, R.A., 1998. Dissecting the regulatory circuitry of a eukaryotic genome. *Cell* 95, 717–728.
- Hubbard, E.J., Greenstein, D., 2000. The *Caenorhabditis elegans* gonad: a test tube for cell and developmental biology. *Dev. Dyn.* 218, 2–22.
- Iwasaki, K., McCarter, J., Francis, R., Schedl, T., 1996. emo-1, a *Caenorhabditis elegans* Sec61p gamma homologue, is required for oocyte development and ovulation. *J. Cell Biol.* 134, 699–714.
- Jaskelioff, M., Gavin, I.M., Peterson, C.L., Logie, C., 2000. SWI-SNF-mediated nucleosome remodeling: role of histone octamer mobility in the persistence of the remodeled state. *Mol. Cell. Biol.* 20, 3058–3068.
- Kaelin Jr., W.G., 1999. Functions of the retinoblastoma protein. *Bioessays* 21, 950–958.
- Kimble, J., Hirsh, D., 1979. The postembryonic cell lineages of the hermaphrodite and male gonads in *Caenorhabditis elegans*. *Dev. Biol.* 70, 396–417.
- Kingston, R.E., Narlikar, G.J., 1999. ATP-dependent remodeling and acetylation as regulators of chromatin fluidity. *Genes Dev.* 13, 2339–2352.
- Krebs, J.E., Fry, C.J., Samuels, M.L., Peterson, C.L., 2000. Global role for chromatin remodeling enzymes in mitotic gene expression. *Cell* 102, 587–598.
- Langst, G., Bonte, E.J., Corona, D.F., Becker, P.B., 1999. Nucleosome movement by CHRAC and ISWI without disruption or trans-displacement of the histone octamer. *Cell* 97, 843–852.
- Lorch, Y., Zhang, M., Kornberg, R.D., 1999. Histone octamer transfer by a chromatin-remodeling complex. *Cell* 96, 389–392.
- Lu, X., Horvitz, H.R., 1998. lin-35 and lin-53, two genes that antagonize a *C. elegans* Ras pathway, encode proteins similar to Rb and its binding protein RbAp48. *Cell* 95, 981–991.
- Luo, R.X., Postigo, A.A., Dean, D.C., 1998. Rb interacts with histone deacetylase to repress transcription. *Cell* 92, 463–473.
- Magnaghi-Jaulin, L., Groisman, R., Naguibneva, I., Robin, P., Lorain, S., Le Villain, J.P., Troalen, F., Trouche, D., Harel-Bellan, A., 1998. Retinoblastoma protein represses transcription by recruiting a histone deacetylase. *Nature* 391, 601–605.
- Markey, M.P., Angus, S.P., Strobeck, M.W., Williams, S.L., Gunawardena, R.W., Aronow, B.J., Knudsen, E.S., 2002. Unbiased analysis of RB-mediated transcriptional repression identifies novel targets and distinctions from E2F action. *Cancer Res.* 62, 6587–6597.
- McCarter, J., Bartlett, B., Dang, T., Schedl, T., 1997. Soma-germ cell interactions in *Caenorhabditis elegans*: multiple events of hermaphrodite germline development require the somatic sheath and spermathecal lineages. *Dev. Biol.* 181, 121–143.
- Mello, C., Fire, A., 1995. DNA transformation. *Methods Cell Biol.* 48, 451–482.
- Miller, M.A., Ruest, P.J., Kosinski, M., Hanks, S.K., Greenstein, D., 2003. An Eph receptor sperm-sensing control mechanism for oocyte meiotic maturation in *Caenorhabditis elegans*. *Genes Dev.* 17, 187–200.
- Morris, E.J., Dyson, N.J., 2001. Retinoblastoma protein partners. *Adv. Cancer Res.* 82, 1–54.
- Myers, C.D., Goh, P.Y., Allen, T.S., Bucher, E.A., Bogaert, T., 1996. Developmental genetic analysis of troponin T mutations in striated and nonstriated muscle cells of *Caenorhabditis elegans*. *J. Cell Biol.* 132, 1061–1077.
- Natarajan, K., Jackson, B.M., Zhou, H., Winston, F., Hinnebusch, A.G., 1999. Transcriptional activation by Gcn4p involves independent interactions with the SWI/SNF complex and the SRB/mediator. *Mol. Cell* 4, 657–664.
- Neely, K.E., Hassan, A.H., Wallberg, A.E., Steger, D.J., Cairns, B.R., Wright, A.P., Workman, J.L., 1999. Activation domain-mediated targeting of the SWI/SNF complex to promoters stimulates transcription from nucleosome arrays. *Mol. Cell* 4, 649–655.
- Nevins, J.R., 1998. Toward an understanding of the functional complexity of the E2F and retinoblastoma families. *Cell Growth Differ.* 9, 585–593.
- Nevins, J.R., 2001. The Rb/E2F pathway and cancer. *Hum. Mol. Genet.* 10, 699–703.
- Newman, A.P., White, J.G., Sternberg, P.W., 1996. Morphogenesis of the *C. elegans* hermaphrodite uterus. *Development* 122, 3617–3626.
- Ng, H.H., Robert, F., Young, R.A., Struhl, K., 2002. Genome-wide location and regulated recruitment of the RSC nucleosome-remodeling complex. *Genes Dev.* 16, 806–819.
- Nielsen, S.J., Schneider, R., Bauer, U.M., Bannister, A.J., Morrison, A., O'Carroll, D., Firestein, R., Cleary, M., Jenuwein, T., Herrera, R.E., Kouzarides, T., 2001. Rb targets histone H3 methylation and HP1 to promoters. *Nature* 412, 561–565.
- Owen-Hughes, T., Utley, R.T., Cote, J., Peterson, C.L., Workman, J.L., 1996. Persistent site-specific remodeling of a nucleosome array by transient action of the SWI/SNF complex. *Science* 273, 513–516.
- Picketts, D.J., Higgs, D.R., Bachoo, S., Blake, D.J., Quarrell, O.W., Gibbons, R.J., 1996. ATRX encodes a novel member of the SNF2 family of proteins: mutations point to a common mechanism underlying the ATR-X syndrome. *Hum. Mol. Genet.* 5, 1899–1907.
- Pradhan, S., Kim, G.D., 2002. The retinoblastoma gene product interacts with maintenance human DNA (cytosine-5) methyltransferase and modulates its activity. *EMBO J.* 21, 779–788.
- Quinn, J., Fyrberg, A.M., Ganster, R.W., Schmidt, M.C., Peterson, C.L., 1996. DNA-binding properties of the yeast SWI/SNF complex. *Nature* 379, 844–847.
- Robertson, K.D., Ait-Si-Ali, S., Yokochi, T., Wade, P.A., Jones, P.L., Wolffe, A.P., 2000. DNMT1 forms a complex with Rb, E2F1 and HDAC1 and represses transcription from E2F-responsive promoters. *Nat. Genet.* 25, 338–342.
- Rose, K.L., Winfrey, V.P., Hoffman, L.H., Hall, D.H., Furuta, T., Greenstein, D., 1997. The POU gene ceh-18 promotes gonadal sheath cell differentiation and function required for meiotic maturation and ovulation in *Caenorhabditis elegans*. *Dev. Biol.* 192, 59–77.
- Russo, G., Claudio, P.P., Fu, Y., Stiegler, P., Yu, Z., Macaluso, M., Giordano, A., 2003. pRB2/p130 target genes in non-small lung cancer cells identified by microarray analysis. *Oncogene* 22, 6959–6969.
- Sawa, H., Kouike, H., Okano, H., 2000. Components of the SWI/SNF complex are required for asymmetric cell division in *C. elegans*. *Mol. Cell* 6, 617–624.
- Schedl, T., 1997. Germ-line development. In: Riddle, D.L., Blumenthal, T., Meyer, B.J., Priess, J.T. (Eds.), *C. elegans* II. Cold Spring Harbor Laboratory Press, Cold Spring Harbor, NY, pp. 241–269.
- Schnitzler, G., Sif, S., Kingston, R.E., 1998. Human SWI/SNF interconverts a nucleosome between its base state and a stable remodeled state. *Cell* 94, 17–27.
- Sherr, C.J., 1996. Cancer cell cycles. *Science* 274, 1672–1677.

- Strober, B.E., Dunaief, J.L., Guha, Goff, S.P., 1996. Functional interactions between the hBRM/hBRG1 transcriptional activators and the pRB family of proteins. *Mol. Cell. Biol.* 16, 1576–1583.
- Sudarsanam, P., Winston, F., 2000. The Swi/Snf family nucleosome-remodeling complexes and transcriptional control. *Trends Genet.* 16, 345–351.
- Sudarsanam, P., Cao, Y., Wu, L., Laurent, B.C., Winston, F., 1999. The nucleosome remodeling complex, Snf/Swi, is required for the maintenance of transcription *in vivo* and is partially redundant with the histone acetyltransferase, Gen5. *EMBO J.* 18, 3101–3106.
- Sudarsanam, P., Iyer, V.R., Brown, P.O., Winston, F., 2000. Whole-genome expression analysis of snf/swi mutants of *Saccharomyces cerevisiae*. *Proc. Natl. Acad. Sci. U. S. A.* 97, 3364–3369.
- Sulston, J., Hodgkin, J., 1988. In: Wood, William B. (Ed.), *The Nematode C. elegans*. Cold Spring Harbor Laboratory Press, Cold Spring Harbor, NY, pp. 587–605.
- Sulston, J.E., Horvitz, H.R., 1977. Post-embryonic cell lineages of the nematode, *Caenorhabditis elegans*. *Dev. Biol.* 56, 110–156.
- Timmons, L., Court, D.L., Fire, A., 2001. Ingestion of bacterially expressed dsRNAs can produce specific and potent genetic interference in *Caenorhabditis elegans*. *Gene* 263, 103–112.
- Tsukiyama, T., 2002. The *in vivo* functions of ATP-dependent chromatin-remodelling factors. *Nat. Rev., Mol. Cell Biol.* 3, 422–429.
- Varga-Weisz, P., 2001. ATP-dependent chromatin remodeling factors: nucleosome shufflers with many missions. *Oncogene* 20, 3076–3085.
- Vernell, R., Helin, K., Muller, H., 2003. Identification of target genes of the p16INK4A-pRB-E2F pathway. *J. Biol. Chem.* 278, 46124–46137.
- Villard, L., Bonino, M.C., Abidi, F., Ragusa, A., Belougne, J., Lossi, A.M., Seaver, L., Bonnefont, J.P., Romano, C., Fichera, M., Lacombe, D., Hanauer, A., Philip, N., Schwartz, C., Fontes, M., 1999. Evaluation of a mutation screening strategy for sporadic cases of ATR-X syndrome. *J. Med. Genet.* 36, 183–186.
- Wallberg, A.E., Neely, K.E., Hassan, A.H., Gustafsson, J.A., Workman, J.L., Wright, A.P., 2000. Recruitment of the SWI-SNF chromatin remodeling complex as a mechanism of gene activation by the glucocorticoid receptor tau1 activation domain. *Mol. Cell. Biol.* 20, 2004–2013.
- Ward, S., Carrel, J.S., 1979. Fertilization and sperm competition in the nematode *Caenorhabditis elegans*. *Dev. Biol.* 73, 304–321.
- Wells, J., Yan, P.S., Cechvala, M., Huang, T., Farnham, P.J., 2003. Identification of novel pRB binding sites using CpG microarrays suggests that E2F recruits pRB to specific genomic sites during S phase. *Oncogene* 22, 1445–1460.
- White-Cooper, H., Leroy, D., MacQueen, A., Fuller, M.T., 2000. Transcription of meiotic cell cycle and terminal differentiation genes depends on a conserved chromatin associated protein, whose nuclear localisation is regulated. *Development* 127, 5463–5473.
- Whitehouse, I., Flaus, A., Cairns, B.R., White, M.F., Workman, J.L., Owen-Hughes, T., 1999. Nucleosome mobilization catalysed by the yeast SWI/SNF complex. *Nature* 400, 784–787.
- Yudkovsky, N., Logie, C., Hahn, S., Peterson, C.L., 1999. Recruitment of the SWI/SNF chromatin remodeling complex by transcriptional activators. *Genes Dev.* 13, 2369–2374.
- Zhang, H.S., Gavin, M., Dahiya, A., Postigo, A.A., Ma, D., Luo, R.X., Harbour, J.W., Dean, D.C., 2000. Exit from G1 and S phase of the cell cycle is regulated by repressor complexes containing HDAC-Rb-hSWI/SNF and Rb-hSWI/SNF. *Cell* 101, 79–89.